Forecasting the Volatility of the Stock Index with Deep Learning Using Asymmetric Hurst Exponents

Poongjin Cho [1] and Minhyuk Lee [2,*]

1   Department of Industrial Engineering, Hanyang University, Seoul 04763, Korea; nadapj@hanyang.ac.kr
2   Department of Business Administration, Pusan National University, Busan 46241, Korea
*   Correspondence: minhyuk.lee@pusan.ac.kr

Abstract: The prediction of the stock price index is a challenge even with advanced deep-learning technology. As a result, the analysis of volatility, which has been widely studied in traditional finance, has attracted attention among researchers. This paper presents a new forecasting model that combines asymmetric fractality and deep-learning algorithms to predict a one-day-ahead absolute return series, the proxy index of stock price volatility. Asymmetric Hurst exponents are measured to capture the asymmetric long-range dependence behavior of the S&P500 index, and recurrent neural network groups are applied. The results show that the asymmetric Hurst exponents have predictive power for one-day-ahead absolute return and are more effective in volatile market conditions. In addition, we propose a new two-stage forecasting model that predicts volatility according to the magnitude of volatility. This new model shows the best forecasting performance regardless of volatility.

Keywords: forecasting; volatility; asymmetry; multifractal; Hurst exponent; deep learning

1. Introduction

Stock price and volatility forecast problems have been studied for a long time in the financial field [1–3], and many studies have recently applied deep-learning techniques to predict the problem [4–6]. Recurrent neural network (RNN) is often used for time-series forecasting in the field of deep learning, which can analyze sequential data using past information [7]. RNN has been widely used to predict stock prices or volatility in the financial field [8–10], and extensively employed in other fields to deal with time-series data [11–13]. However, no matter how predictable the deep-learning technique is, it is difficult to accurately predict stock price and volatility. Therefore, many studies have been conducted to forecast stock volatility [14,15], which is the variance of stock price that can be predicted relatively more accurately than stock price [16–19], while some studies demonstrate the predictive performance of deep-learning algorithms along with domain knowledge in the financial field [20,21].

The generalized Hurst exponent and multifractality are econophysics concepts that inform the characteristics of the time-series, and measure the complexity of the corresponding time-series. They can be measured through multifractal detrended fluctuation analysis (MFDFA) methodology [22], which is one of the most used approaches for estimating multifractality, while the long-range dependence of the time-series can be evaluated with the generalized Hurst exponent. If the long-range dependence of the time-series is different according to the time period, the time-series is known to include multifractality. Conversely, if long-range dependence is the same according to the time period, the time-series is said to be monofractal. If time-series has a multifractality feature, the complexity of the time-series increases, while various stylized factors appear accordingly. The major features of a multifractal are acknowledged to be fat-tail probability distribution, long-term correlation for small and large fluctuations, and volatility clustering. Therefore, if a time-series has a multifractal characteristic, it is likely to have these features. It is generally considered that it

has a long-range dependence if the Hurst exponent of time-series is greater than 0.5, so using this pattern will help predict stock price or stock volatility. Therefore, there have been many efforts to interpret stock price movement through multifractality [23–28]. The application of the pattern is used not only to predict stock price movement, but also to forecast VIX [29], foreign exchange rates [30], and oil price [31]. The authors in Garcin [30] showed that the forecast of foreign exchange rates with time-varying Hurst exponents estimation is effective when the Hurst exponent is over 0.5.

In particular, there are two distinct trends in the stock market—the bull market and the bear market. The asymmetric multifractal detrended fluctuation analysis (A-MFDFA) model [32] distinctly measures the asymmetric multifractal scaling behavior of the generalized Hurst exponent according to these two market trends. Therefore, it appropriately measures the detailed directional generalized Hurst exponent and directional multifractal scale according to stock market conditions. In other words, the A-MFDFA method is the asymmetric generalized Hurst exponent measurement methodology considering the asymmetric nature of stock price movement. In particular, the asymmetric efficiency of the stock market can be estimated with the A-MFDFA according to stock market direction [33]. If the market is not efficient, it implies that the stock market is not a complete random walk and is therefore predictable. As a result, the analysis of the asymmetric Hurst exponents to deal with the predictability has attracted much attention, so that research areas include asymmetric phenomena according to price trend [34–36]. However, little attention has been paid to applying asymmetric multifractal elements to deep learning to forecast the financial market. Therefore, in this study, we predict the stock market with a deep-learning model using the asymmetric Hurst exponent, one of the characteristics of the stock market. Then, we identify whether the asymmetric Hurst exponent is a feature that helps predict the stock market.

Since the price series is non-stationary time-series data, the multifractal concept cannot be applied immediately [37]. This research, therefore, focuses on the prediction of the return series, which is stationary data. Since the multifractal concept or the Hurst exponent is related to the volatility of the return series, it is expected that the Hurst exponent will help predict the volatility of return series. Many volatilities have already been defined in financial markets. For example, historical volatility considers past price movements of the underlying asset, and is also referred to as realized volatility. Implied volatility is a measure of market expectations regarding the asset's future volatility. Parkinson's volatility, which is also called High Low-Range Volatility, aims to estimate volatility using the high and low prices of the day. Garman–Klass volatility calculates daily volatility using more factors (high, low, open, close prices). The VIX Index is based on real-time prices of options on the S&P 500 Index and is designed to reflect investors' consensus views of future (30-day) expected stock market volatility. Each value expresses the volatility of the financial market well; however, in this paper, the absolute value of returns is presented as a proxy of volatility. The reason for this is that it is the easiest way to obtain daily volatility when we only have price series as data. Historical volatility does not focus on only one-day volatility, whereas daily realized volatility needs high-frequency data to compute one-day volatility. Moreover, it is anticipated that asymmetric Hurst exponents are better than the overall Hurst exponent in forecasting the stock market since they have more detailed information of the market situation. Although the volatility of the US stock market is also affected by the volatility of other markets [38], this study focuses on the predictive power of multifractal data of its own US market. In the US stock market, past volatility provides information for future prediction [39]. Therefore, the main subject of this paper is the forecasting of the absolute return series of S&P500 index by applying the asymmetric Hurst exponent to deep learning. First, the asymmetric Hurst exponents are calculated through the close price of the S&P500 index using the A-MFDFA method. Second, along with various RNN models, we predict the absolute return of the S&P500 index for the next day through its past returns and the asymmetric Hurst exponents. Third, we divide the period and investigate the change in forecasting power according to market conditions. Lastly, the new two-stage

forecasting model for the absolute return series is proposed, and the performance of the model is examined by comparing with various benchmarks. The novelty of our study is that it is the first study to predict stock markets using the asymmetric fractality feature as an input to a deep-learning methodology, constructing a new two-stage forecasting model. The results show that asymmetric fractality features are significant in forecasting the stock market. These findings will help investors and regulators to forecast stock markets by revealing the impacts of asymmetric fractality on stock markets.

This paper is organized as follows: Section 2 describes the A-MFDFA methodology for measuring the asymmetric Hurst exponent, and the recurrent neural network model group, which is a deep-learning methodology used for forecasting; Section 3 describes the experimental method and the statistical explanation of the financial data; Section 4 discusses the empirical results of this paper; and Section 5 concludes.

2. Methods

Although there have been many attempts to predict stock price using a neural network, it is no small task since the price series is non-stationary, on the other hand, the prediction of the return, which is a stationary series, is feasible. Since the Hurst exponent is related to the volatility of the return, it is expected to have a major effect in predicting the variant of return by combining it with a neural network. If A-MFDFA considering the market's asymmetric efficiency is combined with a neural network, it is expected that the return will be better predicted.

2.1. Asymmetric Fractality of Stock Price Index

We apply asymmetric fractal scaling behavior for forecasting the financial market for the next day. Then, the asymmetric multifractal detrended fluctuation analysis (A-MFDFA) method is used to measure the asymmetric Hurst exponent, the feature of asymmetric multifractal. The A-MFDFA method is summarized in several steps [32]. Suppose that we have a return time-series $\{x_t : t = 1, 2, \ldots, N\}$ and an index time-series $\{I_t : t = 1, 2, \ldots, N\}$ where $I_t = I_{t-1}exp(x_t) \ for \ t = 1, 2, \ldots, N$.

Step 1: Define the profile of the original time-series as $y_t = \sum_{j=1}^{t}(x_j - \bar{x}), \ t = 1, 2, \ldots, N$ where $\bar{x} = \sum_{j=1}^{N} x_j / N$.

Step 2: Divide the time-series I_t and profile y_t into $N_n(\equiv \lfloor N/n \rfloor)$ non-overlapping sub-time-series of equal length n (scale). This procedure is repeated from the other end of $\{I_t\}$ and $\{y_t\}$, respectively, which yields $2N_n$ sub-time-series. Then, $G_j = \{g_{j,k}, \ k = 1, 2, \ldots, n\}$ be the jth n-length sub-time-series of $\{I_t\}$ and $Y_j = \{y_{j,k}, \ k = 1, 2, \ldots, n\}$ be the jth n-length sub-time-series of $\{y_t\}$ for $j = 1, 2, \ldots, 2N_n$. Please note that $5 \leq n \leq N/4$ [40].

Step 3: For each sub-time-series G_j and Y_j, fit the local linear regression model based on least-squares. $L_{G_j}(k) = a_{G_j} + b_{G_j}k$, and $L_{Y_j}(k) = a_{Y_j} + b_{Y_j}k$, where k be the horizontal coordinate. Then, the sign of b_{G_j} is used to capture the positive or negative local trend of stock market, and $L_{Y_j}(k)$ is used to calculate the fluctuation function, which is defined as

$F_j(n) = \sum_{k=1}^{n} \left(y_{j,k} - L_{Y_j}(k)\right)^2 / n$ for $j = 1, 2, \ldots, 2N_n$.

Step 4: Depending on the sign of b_{G_j}, the asymmetric cross-correlation scaling property of fluctuation functions can be accessed. The directional q-order average fluctuation functions can be defined as $F_q^+(n) = \left(\sum_{j=1}^{2N_n}(1 + sgn(b_{G_j}))\left[F_j(n)\right]^{q/2}/M^+\right)^{1/q}$ and

$F_q^-(n) = \left(\sum_{j=1}^{2N_n}(1 - sgn(b_{G_j}))\left[F_j(n)\right]^{q/2}/M^-\right)^{1/q}$, where $M^+ = \sum_{j=1}^{2N_n}(1 + sgn(b_{G_j}))$, $M^- = \sum_{j=1}^{2N_n}(1 - sgn(b_{G_j}))$ and $sgn(x)$ denote the sign of x. Please note that both b_{G_j} and q are not zero and $M^+ + M^- = 4N_n$. The average fluctuation function of MFDFA model is $F_q(n) = \left(\sum_{j=1}^{2N_n}\left[F_j(n)\right]^{q/2}/(2N_n)\right)^{1/q}$.

Step 5: Calculate the generalized Hurst exponents to capture the asymmetric scaling behavior of the time-series. If time-series possesses the long-range correlation, the following power-law relationship is observed:

$$F_q(n) \propto n^{H_q}, F_q^+(n) \propto n^{H_q^+}, F_q^-(n) \propto n^{H_q^-} \tag{1}$$

where H_q, H_q^+, and H_q^- refer to the overall, up-trend, and down-trend scaling exponents, respectively, and these are also called the generalized Hurst exponents. The generalized Hurst exponents can be determined by the ordinary least square method based on the logarithmic form of power-law relationship in Equation (1).

The time-series is called monofractal when its H_q is unchanged for all q, otherwise it is called multifractal. Furthermore, the correlation in the time-series is anti-persistent when $H_2 < 0.5$, whereas the correlation is persistent when $H_2 > 0.5$. When $H_2 = 0.5$, the time-series follows a random-walk process. In the same context of H_q, the up-trend or down-trend time-series is monofractal or multifractal when its H_q^+ or H_q^- is constant or depends on q, respectively. In addition, the correlation in the time-series is asymmetric if $H_q^+ \neq H_q^-$, whereas the correlation is symmetric if $H_q^+ = H_q^-$. The asymmetric correlation of the time-series means that the asymmetric scaling behavior is different between positive and negative trends.

2.2. Recurrent Neural Network Group

We propose a time-series forecasting based on the asymmetric fractality, which forecasts the financial market for the next day. Specifically, we use four RNN models, which have an advantage in processing time-series data by sequentially processing input values [7]. At first, we employ long short-term memory (LSTM), an updated version of RNN. The LSTM algorithm has a long-term dependency that only remembers important information through a memory cell and forget gate [41]. Therefore, it calculates the hidden state at each time step, which can be obtained as follows:

$$h_t = o_t \odot tanh(c_t) \tag{2}$$

$$c_t = f_t \odot c_{t-1} + i_t \odot tanh(W_y x_t + U_y h_{t-1} + b_y) \tag{3}$$

$$o_t = \sigma(W_o x_t + U_o h_{t-1} + b_o) \tag{4}$$

$$f_t = \sigma(W_f x_t + U_f h_{t-1} + b_f) \tag{5}$$

$$i_t = \sigma(W_i x_t + U_i h_{t-1} + b_i) \tag{6}$$

where h_t, c_t, o_t, f_t, i_t, σ and $\odot$ correspond to the hidden state, memory cell, output gate, forget gate, input gate, sigmoid activation function, and element-wise product, respectively. The model parameters W, U, and b are learned at each time step t.

Second, we use the Gated Recurrent Unit (GRU), a simpler structure than LSTM consisting of reset and update gates [42]. The reset gate properly resets the past information, and the update gate determines the update rate of past and present information, and the two gates are expressed as follows.

$$h_t = (1 - z_t)h_{t-1} + z_t \tilde{h}_t \tag{7}$$

$$\tilde{h}_t = tanh(W_h x_t + U_h(r_t \odot h_{t-1}) + b_h) \tag{8}$$

$$z_t = \sigma(W_z x_t + U_z h_{t-1} + b_z) \tag{9}$$

$$r_t = \sigma(W_r x_t + U_r h_{t-1} + b_r) \tag{10}$$

where $\tilde{h}_t$, z_t, and r_t correspond to the candidate activation, update gate, and reset gate, respectively.

Lastly, we use two more models: the bidirectional long short-term memory (BiLSTM) and bidirectional gated recurrent unit (BiGRU). Both RNNs extract information using two hidden layers in forward direction and reverse direction [43]. The final output of $\mathbf{h}_t$ is as follows:

$$\mathbf{h}_t = [\overrightarrow{h_t} \oplus \overleftarrow{h_t}] \tag{11}$$

where $\overrightarrow{h_t}$, $\overleftarrow{h_t}$ and $\oplus$ represent the output in forward direction, reverse direction, and element-wise sum, respectively [44]. This structure processes data from the past and the future simultaneously, and then the model improves the forecast performance [45].

3. Experiments and Data

3.1. Experiments

For the experiment, we construct the forecast model for an absolute return series of the S&P500 index with asymmetric fractal volatility. A scenario of the proposed forecasting method is illustrated in Figure 1. First, for all periods, the asymmetric Hurst exponents at each time are obtained with the close price. Using the moving-window method, the asymmetric Hurst exponent value of the day is obtained using the data of the past year (252 days). Independent variables consist of returns and the asymmetric Hurst exponents for the last 90 days at each time point, and we normalize the data through min–max scaling. The model predicts the absolute return of the next day based on the normalized data. The data are divided into a training set and test set, while the training set is data from 2000 to 2017, and the test set is data from 2018 to 2020. The model is divided into five types depending on which asymmetric Hurst exponents are added to the independent variable. The first model, which is called 'only_r', predicts the absolute return of the next day through only past returns without the asymmetric Hurst exponents. The second model, which is called 'abs_r', predicts the absolute return of the next day through only past absolute returns without the asymmetric Hurst exponents. The third model, which is called 'his_vol', predicts the one-day-ahead absolute returns through return series and historical volatility. The fourth model, which is called 'H_2', predicts the absolute returns using past return series and overall H_2 (the Hurst exponent) from MFDFA model. The fifth model, which is called 'H_2^+ and H_2^-', forecasts the absolute return through the return series and the asymmetric Hurst exponents (the up-trend Hurst exponent, H_2^+ and the down-trend Hurst exponent, H_2^-) from A-MFDFA model.

The data are entered to the two layers of RNN, and the number of neurons is tuned by Table 1. The output of the second RNN layer is transferred to the two dense layers, predicting the next time step. Each model is trained through four RNNs: LSTM, BiLSTM, GRU, and BiGRU. We find the most suitable model through learning for each model. Hyperparameter tuning is required in each process, and five-cross validation is performed with the hyperparameters in Table 1. We find the model with the best performance based on the validation loss, and the prediction errors of the test data are obtained. For 100 different random seeds, we compare the forecast performances of the four models.
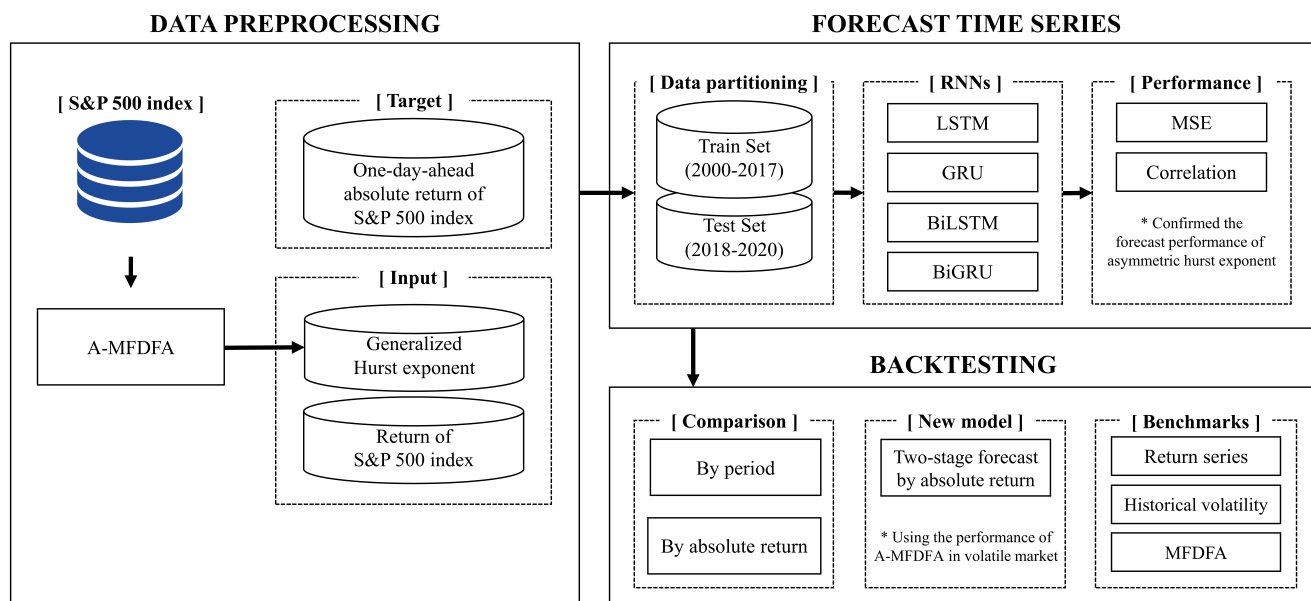
DATA PREPROCESSING

FORECAST TIME SERIES

Figure 1. Proposed forecasting model framework using A-MFDFA with RNNs.

Table 1. Hyperparameter information for the RNN models.

Hyperparameters	Values
Neurons	[25, 50, 100, 200]
Optimizer	Adam
Learning rate	[0.1, 0.01, 0.001]
Epochs	[25, 50, 100]
Batch size	[50, 100, 200, 400, 800]

3.2. Data

To forecast the one-day-ahead absolute return of S&P500 index, we use return series for the past 90 days. Please note that we apply min–max scaling. To show that the asymmetric fractality of the stock market has a predictive power, four fractal elements are constructed, which are as follows: historical volatility, overall Hurst exponent H_2, up-trend Hurst exponent H_2^+, and down-trend Hurst exponent H_2^-.

S&P500 index data are used to forecast the one-day-ahead absolute return, and Table 2 shows the data statistics of S&P500 index data. Daily return series for the S&P500 is denoted by r, and $|r|$ denotes the daily absolute return series for the S&P500, which is the proxy index of the daily return volatility. his_vol is the standard deviation of the past 20 days. Figure 2 shows the overall, up-trend, and down-trend Hurst exponents in the form of time-series data. The data period is from 2000 to 2020. As a result of the Jarque–Bera (JB) test, all series in Table 2 are not the normal distribution with a significant level of 1%. The absence of unit root is rejected with 1% significant level as a result of the Augmented Dickey–Fuller (ADF) test. Therefore, all time-series are stationary.

Table 2. Data statistics.

	Mean	Max	Min	Standard Deviation	Skewness	Kurtosis	Jarque–Bera Test	ADF Test [1]
r	0.0003	0.1158	−0.1198	0.0125	−0.17	11.43	27,402.2 *	−17.1 *
$\|r\|$	0.0081	0.1198	0	0.0095	3.59	22.54	117,313.6 *	−6.6 *
his_vol	0.0044	0.0261	0.0009	0.0030	3.14	14.21	50,586.1 *	−6.2 *
H_2	0.4731	0.6022	0.3158	0.0478	−0.25	−0.41	87.8 *	−3.7 *
H_2^+	0.4398	0.7385	−0.0542	0.1020	−1.03	2.54	2234.6 *	−4.3 *
H_2^-	0.4964	0.8643	0.0399	0.0847	−0.49	2.14	1163.7 *	−5.3 *

[1] denotes Augmented Dickey–Fuller Test, and * denotes 1% level of significance.
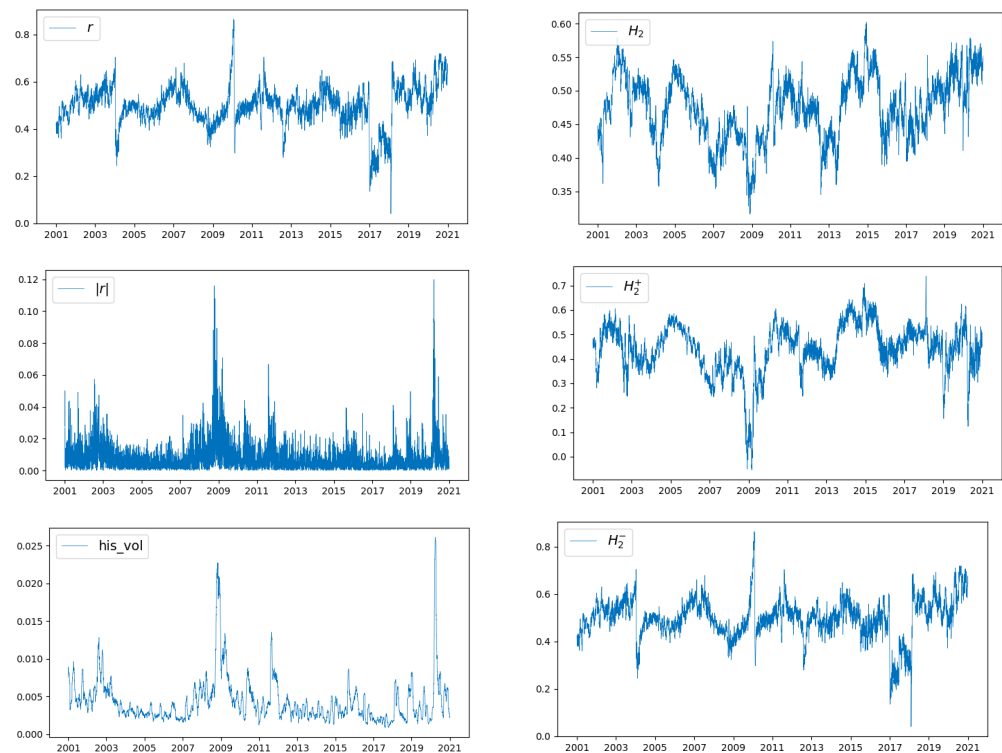

Figure 2. The graph of time-series data for daily return, absolute return, historical volatility and overall, up-trend, down-trend Hurst exponents of S&P500 index data from 2000 to 2020.

4. Results

4.1. Forecasting Performance by Model

As previously stated, we use the multifractal elements of MFDFA and A-MFDFA to forecast the absolute return series of S&P500 index. To prove that the Hurst exponents have a predictive power, we predict the absolute return from 2018 to 2020 using four RNNs (LSTM, BiLSTM, GRU, BiGRU). To compare the performance of the forecast result, five performance metrics are used: mean forecast error (MFE), mean squared error (MSE), mean absolute percentage error (MAPE), relative absolute error (RAE), and correlation coefficient (*r*). MFE, MSE, MAPE, and RAE are common metrics for evaluating the performance of regression, and the correlation coefficient measures the linear relationship between two time-series. The lower the MSE, MAPE, and RAE, the lower the absolute value of MFE, and the higher *r*, the better the predictive performance of the model. We can employ the values to compare the actual and the predicted values, which are calculated as:

$$\text{MFE} = \frac{1}{n}\sum_{i=1}^{n}(x_i - y_i) \tag{12}$$

$$\text{MSE} = \frac{1}{n} \sum_{i=1}^{n} (x_i - y_i)^2 \tag{13}$$

$$\text{MAPE} = \frac{1}{n} \sum_{i=1}^{n} \frac{|x_i - y_i|}{x_i} \tag{14}$$

$$\text{RAE} = \frac{[\sum_{i=1}^{n} (x_i - y_i)^2]^{\frac{1}{2}}}{[\sum_{i=1}^{n} x_i^2]^{\frac{1}{2}}} \tag{15}$$

$$r = \frac{\sum_{i=1}^{n} (x_i - \bar{x})(y_i - \bar{y})}{\sqrt{\sum_{i=1}^{n} (x_i - \bar{x})^2} \sqrt{\sum_{i=1}^{n} (y_i - \bar{y})^2}} \tag{16}$$

where x_i and y_i represent the actual and predicted value, respectively. $\bar{x}$ and $\bar{y}$ denote the average of the actual and forecast value, respectively. The MFE, MSE, MAPE, RAE, and the correlation coefficient between the actual value and predicted value are obtained, and they are shown in Table 3.

Since the return series is stationary unlike the price series, predicting tomorrow's absolute return as today's absolute return has fairly predictive power. If a one-day-ahead absolute return from 2018 to 2020 is predicted as today's absolute return, an MSE of 0.000140 is obtained, which is 29.6% higher than 0.000108, with the result predicted by LSTM using only return series. Therefore, RNN can better predict the stationary absolute return series.
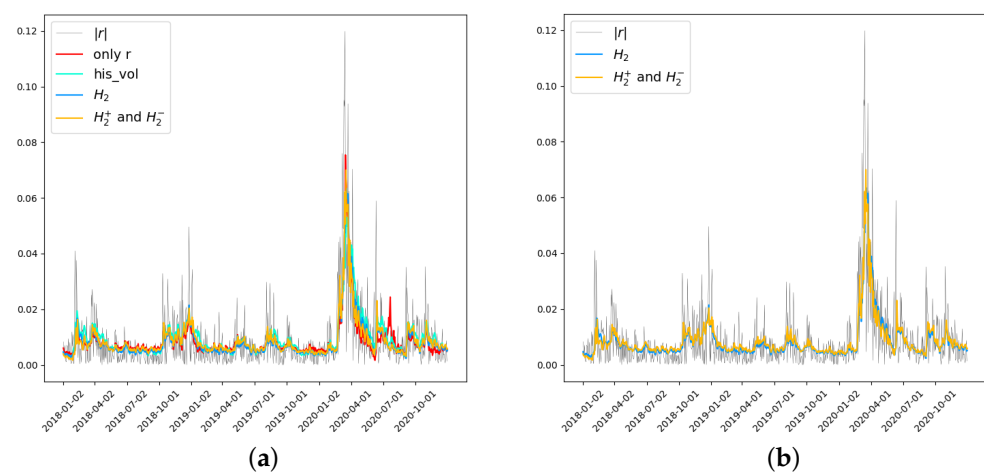
The absolute value of returns is presented as a proxy of volatility. The most basic method of computing volatility of return is historical volatility. Since it does not only focus on one day, it is not a very good estimate of daily volatility, whereas realized volatility uses high-frequency data to compute a one-day volatility. The predictive power of historical volatility can be compared with the asymmetric Hurst exponents. According to Table 3, when forecasting with all four RNNs, the predictive power of historical volatility is lower than that of all asymmetric Hurst exponents. Therefore, in predicting an absolute return series, forecasting power can be enhanced through the asymmetric Hurst exponents rather than historical volatility.

We obtain three values of Hurst exponents through the A-MFDFA model. We compare which element has more predictive power in forecasting the absolute return series among the three Hurst exponents. According to Table 3, with all four RNNs, the predictive power of the overall Hurst exponent (H_2) is lower than that of the up–down Hurst exponents (H_2^+ and H_2^-). Therefore, in forecasting the absolute return series, the predictive power of the asymmetric Hurst exponents (H_2^+ and H_2^-) using the A-MFDFA method is better than that of the overall Hurst exponent (H_2) using the MFDFA method.

Figure 3 compares the predicted value of each model with the actual absolute return. Each model predicts the trend of absolute return well, and forecasts the trend appropriately even in the situation of the COVID-19 pandemic shock in early 2020.

Table 3. Forecasting the performance of four RNN models with different inputs from 2018 to 2020 (Please note that: the best results are highlighted in **BOLD**).

RNNs	Mean Forecast Error (MFE)				
	only_r	abs_r	his_vol	H_2	H_2^+ and H_2^-
LSTM	0.001991	0.000550	−0.000496	0.000535	**0.000222**
BiLSTM	0.001281	**−0.000175**	0.000985	0.000367	0.000355
GRU	0.001170	**0.000063**	0.000527	−0.000093	−0.000088
BiGRU	0.000417	0.000326	0.000479	−0.000279	**−0.000153**

RNNs	Mean Squared Error (MSE)				
	only_r	abs_r	his_vol	H_2	H_2^+ and H_2^-
LSTM	0.000108	0.000090	0.000082	0.000078	**0.000074**
BiLSTM	0.000108	0.000090	0.000083	0.000081	**0.000075**
GRU	0.000083	0.000089	0.000083	0.000081	**0.000076**
BiGRU	0.000083	0.000088	0.000084	0.000080	**0.000078**

RNNs	Mean Absolute Percentage Error (MAPE)				
	only_r	abs_r	his_vol	H_2	H_2^+ and H_2^-
LSTM	5.179741	**4.620230**	5.429739	4.785479	5.239507
BiLSTM	5.860047	5.236483	**4.067028**	4.830518	5.101785
GRU	4.668557	5.116752	**4.647369**	4.995071	5.157459
BiGRU	5.239868	4.761588	**4.574991**	5.102364	5.371415

RNNs	Relative Absolute Error (RAE)				
	only_r	abs_r	his_vol	H_2	H_2^+ and H_2^-
LSTM	0.706238	0.645170	0.615501	0.600626	**0.583254**
BiLSTM	0.706757	0.644208	0.618452	0.610441	**0.589258**
GRU	0.619729	0.639924	0.618881	0.611304	**0.591806**
BiGRU	0.622382	0.638673	0.621853	0.609870	**0.600117**

RNNs	Correlation Coefficient (*r*)				
	only_r	abs_r	his_vol	H_2	H_2^+ and H_2^-
LSTM	0.575273	0.588556	0.637340	0.659337	**0.685704**
BiLSTM	0.559028	0.588571	0.636998	0.643334	**0.676700**
GRU	0.636332	0.595553	0.632082	0.641523	**0.675415**
BiGRU	0.626024	0.598658	0.626373	0.643753	**0.672501**

Figure 3. Forecast performance of absolute return. (**a**) All models. (**b**) Multifractal models.

4.2. Forecasting Performance by Period

The market condition from 2018 to 2020, the period of the test set, is affected by COVID-19. Therefore, it is necessary to observe how the forecast performance changes by dividing the detailed period since the forecast performance can be greatly affected by the market conditions, COVID-19. As a result, the test set is divided into three sections for each year, and the performance of the model for each period is calculated as shown in Table 4 to compare the forecasting performance according to each period. Among the predicted values obtained through the four RNNs, the values with the highest performance are specified.

Table 4. Forecasting performance by period with different inputs (Please note that the best results are highlighted in **BOLD**).

Test period	Mean Forecast Error (MFE)				
	only r	abs_r	his_vol	H_2	H_2^+ and H_2^-
2018~2020	0.000417	−0.000175	−0.000496	−0.000279	**−0.000153**
2018	−0.000811	**−0.000102**	−0.000831	−0.000207	−0.000263
2019	−0.001465	−0.000881	−0.001133	**−0.000565**	−0.001031
2020	0.002368	0.000460	0.000481	**−0.000177**	0.000583

Test period	Mean Squared Error (MSE)				
	only r	abs_r	his_vol	H_2	H_2^+ and H_2^-
2018~2020	0.000083	0.000088	0.000082	0.000078	**0.000074**
2018	0.000048	0.000056	0.000048	**0.000047**	0.000047
2019	0.000024	0.000027	0.000025	**0.000023**	0.000024
2020	0.000178	0.000182	0.000172	0.000164	**0.000147**

Test period	Mean Absolute Percentage Error (MAPE)				
	only r	abs_r	his_vol	H_2	H_2^+ and H_2^-
2018~2020	4.668557	4.620230	**4.067028**	4.785479	5.101785
2018	6.815235	5.507806	**5.114793**	6.680978	6.936253
2019	5.582146	5.977801	**4.980626**	5.675435	6.080174
2020	**1.321910**	2.366138	2.007365	1.967344	1.950882

Test period	Relative Absolute Error (RAE)				
	only r	abs_r	his_vol	H_2	H_2^+ and H_2^-
2018~2020	0.619729	0.638673	0.615501	0.600626	**0.583254**
2018	0.645257	0.698807	0.645018	**0.637218**	0.641716
2019	0.616997	0.656017	0.628997	**0.608554**	0.614759
2020	0.613622	0.620194	0.603294	0.589567	**0.558003**

Test period	Correlation Coefficient (r)				
	only r	abs_r	his_vol	H_2	H_2^+ and H_2^-
2018~2020	0.559028	0.588556	0.626373	0.641523	**0.672501**
2018	**0.452544**	0.271690	0.445440	0.452020	0.390719
2019	0.463970	0.341053	0.404548	**0.485692**	0.484991
2020	0.631301	0.597044	0.623261	0.635442	**0.682741**

According to Table 4, the model of up–down Hurst exponents (H_2^+ and H_2^-) performs the best for MFE, MSE, RAE, and *r* in all test periods (2018~2020). In 2018 and 2019, however, it can be seen that the predictive power of overall Hurst exponent (H_2) model is higher than that of up–down Hurst exponents (H_2^+ and H_2^-) model for all five performance metrics. In 2020, as the period affected by the COVID-19 in a crisis, the up–down Hurst exponents (H_2^+ and H_2^-) model achieves the best performance for MSE, RAE, and *r*, while the volatility of the market is very large. Moreover, the predictive power of up–down Hurst exponents (H_2^+ and H_2^-) model is better than that of overall Hurst exponent (H_2) model

for four performance metrics since up–down Hurst exponents consider the asymmetric market situation. In other words, when the market volatility is small, the overall Hurst exponent (H_2) has slightly better predictive power; however, when the volatility is large, the asymmetric Hurst exponents (H_2^+ and H_2^-) have much better predictive power.

We conclude that the better forecasting results from asymmetric Hurst exponents (H_2^+ and H_2^-) in 2020 are in response to the volatile market by COVID-19. Therefore, we investigate whether the forecasting results using asymmetric Hurst exponents are predictable if the market is volatile. To prove whether there is an actual difference in predictive power according to the magnitude of the volatility, MFE, MSE, MAPE, RAE, and r are calculated according to the magnitude of absolute return as shown in Table 5. Among the predicted values obtained through the four RNNs, the values with the highest performance are specified. The magnitude of the absolute return is divided by 0.01 units to investigate the forecasting performance of the model for each interval. As a result, when the absolute return is 0.01 or more, the forecasting performance of up–down Hurst exponents (H_2^+ and H_2^-) is high, while the highest performance is obtained in four intervals for MSE and RAE, and three intervals for MAPE. Therefore, when the market is volatile, the up–down Hurst exponents (H_2^+ and H_2^-) are expected to have better predictive power.

Table 5. Forecasting performance by absolute return with different inputs (Please note that: the best results are highlighted in **BOLD**).

$|r|$	Mean Forecast Error (MFE)				
	only r	abs_r	his_vol	H_2	H_2^+ and H_2^-
[0.05, ∞)	**0.035077**	0.039647	0.040481	0.035353	0.035279
[0.04, 0.05)	0.020548	0.021101	0.019323	**0.015931**	0.016033
[0.03, 0.04)	0.018455	0.015994	**0.015626**	0.015897	0.017917
[0.02, 0.03)	0.012032	0.010949	0.008980	**0.008744**	0.009469
[0.01, 0.02)	0.004302	0.003037	**0.001996**	0.002598	0.002950
[0, 0.01]	−0.001985	−0.002574	**−0.001858**	−0.002427	−0.002720
$|r|$	Mean Squared Error (MSE)				
	only r	abs_r	his_vol	H_2	H_2^+ and H_2^-
[0.05, ∞)	0.002117	0.002187	0.002202	0.001943	**0.001831**
[0.04, 0.05)	0.000606	0.000728	0.000507	0.000477	**0.000391**
[0.03, 0.04)	0.000446	0.000430	**0.000368**	0.000382	0.000394
[0.02, 0.03)	0.000216	0.000200	0.000160	0.000178	**0.000153**
[0.01, 0.02)	0.000044	0.000052	0.000042	0.000048	**0.000033**
[0, 0.01]	**0.000015**	0.000027	0.000025	0.000026	0.000026
$|r|$	Mean Absolute Percentage Error (MAPE)				
	only r	abs_r	his_vol	H_2	H_2^+ and H_2^-
[0.05, ∞)	0.531546	0.487245	0.487680	**0.454895**	0.491992
[0.04, 0.05)	0.516462	0.551105	0.458238	0.450806	**0.395999**
[0.03, 0.04)	0.587881	0.561016	**0.495632**	0.517947	0.550990
[0.02, 0.03)	0.574537	0.545820	0.469157	0.489975	**0.465984**
[0.01, 0.02)	0.398782	0.380984	0.348474	0.389920	**0.338659**
[0, 0.01]	6.278127	6.221458	**5.463714**	6.459031	6.900582
$|r|$	Relative Absolute Error (RAE)				
	only r	abs_r	his_vol	H_2	H_2^+ and H_2^-
[0.05, ∞)	0.569846	0.579202	0.581125	0.545842	**0.529862**
[0.04, 0.05)	0.540665	0.592765	0.494642	0.479969	**0.434611**
[0.03, 0.04)	0.636086	0.624674	**0.578241**	0.588744	0.597860
[0.02, 0.03)	0.604180	0.580934	0.519819	0.548542	**0.508595**
[0.01, 0.02)	0.473051	0.510815	0.462224	0.490842	**0.407824**
[0, 0.01]	**0.799368**	1.069389	1.017264	1.031607	1.036734

Table 5. *Cont.*

$|r|$	Correlation Coefficient (r)				
	only r	abs_r	his_vol	H_2	H_2^+ and H_2^-
$[0.05, \infty)$	0.225248	−0.010060	0.052341	0.163925	**0.237050**
$[0.04, 0.05)$	**0.484073**	−0.028696	0.110229	0.077351	0.324021
$[0.03, 0.04)$	**0.194590**	0.023705	−0.048152	−0.022601	−0.034044
$[0.02, 0.03)$	0.205409	**0.275913**	0.188228	0.264143	0.273881
$[0.01, 0.02)$	0.128505	0.078567	0.106038	0.137721	**0.182979**
$[0, 0.01]$	0.101981	0.116562	0.113245	0.127867	**0.135427**

4.3. Constructing a New Two-Stage Forecasting Model Using Asymmetric Hurst Exponents

The above result in Section 4.1 may simply suggest that the model of only r tends to predict low, and the model of up–down Hurst exponents (H_2^+ and H_2^-) tends to predict high. Moreover, according to the result of Section 4.2, up–down Hurst exponents (H_2^+ and H_2^-) have more predictive power than other models in a highly volatile period. Therefore, with the features of the models, we propose a new two-stage forecasting model according to the magnitude of volatility using the asymmetric Hurst exponents as follows. This model forecasts the one-day-ahead absolute return through overall Hurst exponent (H_2) if the magnitude of the absolute return of the previous day is less than 0.02. Conversely, if the magnitude of the previous day's absolute return is 0.02 or more, forecasting is made through up–down Hurst exponents (H_2^+ and H_2^-). The results are in Table 6, among the predicted values obtained through the four RNNs, the values with the highest performance are specified. It shows slightly lower predictive power than up–down Hurst exponents (H_2^+ and H_2^-) in 2020, but higher predictive power than all models for 2018~2020, 2018, and 2019. These results also show that the up–down Hurst exponents (H_2^+ and H_2^-) are more predictive in volatile markets. The Diebold–Mariano test [46] is performed to investigate how different the predicted values of the developed model are from those of the existing model. The DM (Diebold–Mariano) value for the predicted value is obtained for each test period, and the result is as shown in Table 7. In 2018, the new two-stage forecasting model is not significantly different from overall Hurst exponent (H_2) and up–down Hurst exponents (H_2^+ and H_2^-), which means the market includes both stable and unstable periods. In 2019, however, the two-stage model is statistically different from up–down Hurst exponents (H_2^+ and H_2^-), which implies the stable period. In 2020, on the other hand, the new model is significantly different from overall Hurst exponent (H_2), which indicates the volatile period. For the entire period, the new model cannot reject the assumption that it is statistically different from the up–down Hurst exponents (H_2^+ and H_2^-), but when examined by period, it rejects the assumption for 2019.

Table 6. Forecasting performance by period with new two-stage model (Please note that the best results are highlighted in **BOLD**).

Test period	Mean Forecast Error (MFE)					
	only r	abs_r	his_vol	H_2	H_2^+ and H_2^-	new two-stage forecasting model
2018~2020	0.000417	−0.000175	−0.000496	−0.000279	**−0.000153**	0.000449
2018	−0.000811	**−0.000102**	−0.000831	−0.000207	−0.000263	−0.000234
2019	−0.001465	−0.000881	−0.001133	−0.000565	−0.001031	**−0.000398**
2020	0.002368	0.000460	0.000481	**−0.000177**	0.000583	0.001983

Table 6. *Cont.*

Test period	Mean Squared Error (MSE)					
	only r	abs_r	his_vol	H_2	H_2^+ and H_2^-	new two-stage forecasting model
2018~2020	0.000083	0.000088	0.000082	0.000078	0.000074	**0.000073**
2018	0.000048	0.000056	0.000048	0.000047	0.000047	**0.000046**
2019	0.000024	0.000027	0.000025	0.000023	0.000024	**0.000023**
2020	0.000178	0.000182	0.000172	0.000164	**0.000147**	0.000148

Test period	Mean Absolute Percentage Error (MAPE)					
	only r	abs_r	his_vol	H_2	H_2^+ and H_2^-	new two-stage forecasting model
2018~2020	4.668557	4.620230	**4.067028**	4.785479	5.101785	4.853296
2018	6.815235	5.507806	**5.114793**	6.680978	6.936253	6.788785
2019	5.582146	5.977801	**4.980626**	5.675435	6.080174	5.827391
2020	**1.321910**	2.366138	2.007365	1.967344	1.950882	1.939831

Test period	Relative Absolute Error (RAE)					
	only r	abs_r	his_vol	H_2	H_2^+ and H_2^-	new two-stage forecasting model
2018~2020	0.619729	0.638673	0.615501	0.600626	0.583254	**0.578949**
2018	0.645257	0.698807	0.645018	0.637218	0.641716	**0.636665**
2019	0.616997	0.656017	0.628997	0.608554	0.614759	**0.605353**
2020	0.613622	0.620194	0.603294	0.589567	**0.558003**	0.560339

Test period	Correlation Coefficient (*r*)					
	only r	abs_r	his_vol	H_2	H_2^+ and H_2^-	new two-stage forecasting model
2018~2020	0.559028	0.588556	0.626373	0.641523	0.672501	**0.692084**
2018	0.452544	0.271690	0.445440	0.452020	0.390719	**0.472469**
2019	0.463970	0.341053	0.404548	0.485692	0.484991	**0.510441**
2020	0.631301	0.597044	0.623261	0.635442	0.682741	**0.708169**

Table 7. Diebold–Mariano test of new two-stage forecasting model.

Test period	Model 1	Model 2	DM	*p*-value
2018	new two-stage forecasting model	only r	0.40851	0.6832
		abs_r	2.138974	0.0334
		his_vol	1.636703	0.1029
		H_2	1.289953	0.1983
		H_2^+ and H_2^-	0.662737	0.5081

Test period	Model 1	Model 2	DM	*p*-value
2019	new two-stage forecasting model	only r	−1.148275	0.2519
		abs_r	2.368063	0.0186
		his_vol	3.851128	0.0001
		H_2	−1.096094	0.2741
		H_2^+ and H_2^-	2.496623	0.0132

Test period	Model 1	Model 2	DM	*p*-value
2020	new two-stage forecasting model	only r	1.987767	0.0479
		abs_r	3.082361	0.0023
		his_vol	2.274708	0.0238
		H_2	2.093985	0.0373
		H_2^+ and H_2^-	0.376932	0.7065

Table 7. *Cont.*

Test period	Model 1	Model 2	DM	*p*-value
2018~2020	new two-stage forecasting model	only r	1.620336	0.1056
		abs_r	4.286774	0.0000
		his_vol	3.815629	0.0001
		H_2	2.196733	0.0283
		H_2^+ and H_2^-	1.766298	0.0778

5. Discussion and Conclusions

The volatility forecasting problem in the stock market has been one of the most important research topics in finance. In this paper, we predict the absolute return series, the proxy index of volatility, using asymmetric fractality features with deep-learning algorithms. The asymmetric Hurst exponents are used to capture the asymmetric long-range dependence behavior of the financial market and recurrent neural network groups are employed in the forecasting model. These prediction methodologies are applied to the S&P500 index to check whether the methodologies perform better than other benchmarks.

First, we construct a volatility prediction model using five types of input variable. The first type uses only past returns for the input variables. The second type uses absolute returns. The third type uses past returns and historical volatility. The fourth type uses past returns and the overall Hurst exponent, and the fifth type takes past returns and the asymmetric Hurst exponents as input variables. Each model is trained using four RNNs: LSTM, BiLSTM, GRU, and BiGRU. The results demonstrate that the model using the asymmetric Hurst exponent performs the best. It implies that asymmetric Hurst exponents have predictive power for one-day-ahead absolute return. To further prove the predictability of the model, we conduct sub-period analysis. As a result, predictive power is similar in the period of low volatility; however, the model using asymmetric Hurst exponents has the highest predictive power in 2020, when volatility is highest in response to COVID-19. This means that the asymmetric nature of stock price movement has greater predictive power in volatile market conditions, so that it could be better proven in the context of COVID-19. Applying the implication, we finally propose a new two-stage forecasting model that forecasts volatility by dividing conditions according to the magnitude of volatility. It shows similar performance to up–down Hurst exponents (H_2^+ and H_2^-) in 2020, but better predictive power in terms of MSE, MAPE, RAE, and *r* in 2018, 2019, and 2018~2020. Therefore, the new model achieves the best prediction performance regardless of the magnitude of volatility. The new model decides whether to use overall Hurst exponent (H_2) or up–down Hurst exponents (H_2^+ and H_2^-) based on the previous day's absolute return value of 0.02; however, it is possible to use more past information or fine-tune the parameters of absolute returns.

The novelty of our study is that it is the first to predict stock markets using the asymmetric fractal factor as an input to deep-learning methodology. The two-stage forecasting model using the asymmetric fractal factor demonstrates high predictive power in volatile market conditions. These findings will help investors and regulators to forecast stock markets by revealing the impacts of asymmetric fractality on stock markets. It would be helpful to design a model by combining the asymmetric fractal with several other variables such as financial market variables and macroeconomic variables that affect stock volatility. In this study, a model combining the overall Hurst exponent and the asymmetric Hurst exponent is proposed using the conclusion that the asymmetric Hurst exponent is suitable for the volatile market. In future studies, various other measures of stock volatility such as realized volatility or Garman–Klass volatility can be used; moreover, density forecast that predicts the overall distribution can be compared.

References

1. Sezer, O.B.; Gudelek, M.U.; Ozbayoglu, A.M. Financial time series forecasting with deep learning: A systematic literature review: 2005–2019. *Appl. Soft Comput.* **2020**, *90*, 106181. [CrossRef]
2. Pai, P.F.; Lin, C.S. A hybrid ARIMA and support vector machines model in stock price forecasting. *Omega* **2005**, *33*, 497–505. [CrossRef]
3. Hadavandi, E.; Shavandi, H.; Ghanbari, A. Integration of genetic fuzzy systems and artificial neural networks for stock price forecasting. *Knowl.-Based Syst.* **2010**, *23*, 800–808. [CrossRef]
4. Qiu, M.; Song, Y.; Akagi, F. Application of artificial neural network for the prediction of stock market returns: The case of the Japanese stock market. *Chaos Solitons Fractals* **2016**, *85*, 1–7. [CrossRef]
5. Althelaya, K.A.; El-Alfy, E.S.M.; Mohammed, S. Stock Market Forecast Using Multivariate Analysis with Bidirectional and Stacked (LSTM, GRU). In Proceedings of the 2018 21st Saudi Computer Society National Computer Conference (NCC), Riyadh, Saudi Arabia, 25–26 April 2018; pp. 1–7. [CrossRef]
6. Sethia, A.; Raut, P. Application of LSTM, GRU and ICA for Stock Price Prediction. In *Information and Communication Technology for Intelligent Systems*; Satapathy, S.C., Joshi, A., Eds.; Springer: Singapore, 2019; pp. 479–487. [CrossRef]
7. Connor, J.; Martin, R.; Atlas, L. Recurrent neural networks and robust time series prediction. *IEEE Trans. Neural Netw.* **1994**, *5*, 240–254. [CrossRef] [PubMed]
8. Lahmiri, S.; Bekiros, S. Cryptocurrency forecasting with deep learning chaotic neural networks. *Chaos Solitons Fractals* **2019**, *118*, 35–40. [CrossRef]
9. Liang, L.; Cai, X. Forecasting peer-to-peer platform default rate with LSTM neural network. *Electron. Commer. Res. Appl.* **2020**, *43*, 100997. [CrossRef]
10. Li, Y.; Jiang, S.; Li, X.; Wang, S. The role of news sentiment in oil futures returns and volatility forecasting: Data-decomposition based deep learning approach. *Energy Econ.* **2021**, *95*, 105140. [CrossRef]
11. Shahid, F.; Zameer, A.; Muneeb, M. Predictions for COVID-19 with deep learning models of LSTM, GRU and Bi-LSTM. *Chaos Solitons Fractals* **2020**, *140*, 110212. [CrossRef]
12. Chimmula, V.K.R.; Zhang, L. Time series forecasting of COVID-19 transmission in Canada using LSTM networks. *Chaos Solitons Fractals* **2020**, *135*, 109864. [CrossRef]
13. Fu, R.; Zhang, Z.; Li, L. Using LSTM and GRU neural network methods for traffic flow prediction. In Proceedings of the 2016 31st Youth Academic Annual Conference of Chinese Association of Automation (YAC), Wuhan, China, 11–13 November 2016; pp. 324–328. [CrossRef]
14. Gong, X.L.; Liu, X.H.; Xiong, X.; Zhuang, X.T. Forecasting stock volatility process using improved least square support vector machine approach. *Soft Comput.* **2019**, *23*, 11867–11881. [CrossRef]
15. Wang, Z.; Bouri, E.; Ferreira, P.; Shahzad, S.J.H.; Ferrer, R. A grey-based correlation with multi-scale analysis: S&P 500 VIX and individual VIXs of large US company stocks. *Financ. Res. Lett.* **2022**, *48*, 102872. [CrossRef]
16. Sardelich, M.; Manandhar, S. Multimodal deep learning for short-term stock volatility prediction. *arXiv* **2018**, arXiv:1812.10479.
17. Kim, H.Y.; Won, C.H. Forecasting the volatility of stock price index: A hybrid model integrating LSTM with multiple GARCH-type models. *Expert Syst. Appl.* **2018**, *103*, 25–37. [CrossRef]
18. Chen, S.; Zhang, Z. Forecasting Implied Volatility Smile Surface via Deep Learning and Attention Mechanism. *arXiv* **2019**, arXiv:1912.11059.
19. Liu, Y. Novel volatility forecasting using deep learning–Long Short Term Memory Recurrent Neural Networks. *Expert Syst. Appl.* **2019**, *132*, 99–109. [CrossRef]
20. Hu, Y.; Ni, J.; Wen, L. A hybrid deep learning approach by integrating LSTM-ANN networks with GARCH model for copper price volatility prediction. *Phys. A Stat. Mech. Its Appl.* **2020**, *557*, 124907. [CrossRef]
21. Jiang, M.; Liu, J.; Zhang, L.; Liu, C. An improved Stacking framework for stock index prediction by leveraging tree-based ensemble models and deep learning algorithms. *Phys. A Stat. Mech. Its Appl.* **2020**, *541*, 122272. [CrossRef]
22. Kantelhardt, J.W.; Zschiegner, S.A.; Koscielny-Bunde, E.; Havlin, S.; Bunde, A.; Stanley, H. Multifractal detrended fluctuation analysis of nonstationary time series. *Phys. A Stat. Mech. Its Appl.* **2002**, *316*, 87–114. [CrossRef]

23. Yuan, Y.; Zhang, T. Forecasting stock market in high and low volatility periods: A modified multifractal volatility approach. *Chaos Solitons Fractals* **2020**, *140*, 110252. [CrossRef]

24. Li, Y.; Vilela, A.L.; Stanley, H.E. The institutional characteristics of multifractal spectrum of China's stock market. *Phys. A Stat. Mech. Its Appl.* **2020**, *550*, 124129. [CrossRef]

25. Wang, L.; Liu, L. Long-range correlation and predictability of Chinese stock prices. *Phys. A Stat. Mech. Its Appl.* **2020**, *549*, 124384. [CrossRef]

26. Choi, S.Y. Analysis of stock market efficiency during crisis periods in the US stock market: Differences between the global financial crisis and COVID-19 pandemic. *Phys. A Stat. Mech. Its Appl.* **2021**, *574*, 125988. [CrossRef]

27. Aslam, F.; Ferreira, P.; Mohti, W. Investigating efficiency of frontier stock markets using multifractal detrended fluctuation analysis. *Int. J. Emerg. Mark.* **2021**. [CrossRef]

28. Shahzad, S.J.H.; Bouri, E.; Kayani, G.M.; Nasir, R.M.; Kristoufek, L. Are clean energy stocks efficient? Asymmetric multifractal scaling behaviour. *Phys. A Stat. Mech. Its Appl.* **2020**, *550*, 124519. [CrossRef]

29. Bianchi, S.; Di Sciorio, F.; Mattera, R. Forecasting VIX with Hurst Exponent. In *Mathematical and Statistical Methods for Actuarial Sciences and Finance*; Corazza, M., Perna, C., Pizzi, C., Sibillo, M., Eds.; Springer International Publishing: Cham, Switzerland, 2022; pp. 90–95. [CrossRef]

30. Garcin, M. Estimation of time-dependent Hurst exponents with variational smoothing and application to forecasting foreign exchange rates. *Phys. A Stat. Mech. Its Appl.* **2017**, *483*, 462–479. [CrossRef]

31. Lin, Y.; Han, D.; Du, J.; Jia, G. The Mechanism of Google Trends Affecting Crude Oil Price Forecasting. *SN Comput. Sci.* **2022**, *3*, 1–12. [CrossRef]

32. Lee, M.; Song, J.W.; Park, J.H.; Chang, W. Asymmetric multi-fractality in the U.S. stock indices using index-based model of A-MFDFA. *Chaos Solitons Fractals* **2017**, *97*, 28–38. [CrossRef]

33. Lee, M.; Song, J.W.; Kim, S.; Chang, W. Asymmetric market efficiency using the index-based asymmetric-MFDFA. *Phys. A Stat. Mech. Its Appl.* **2018**, *512*, 1278–1294. [CrossRef]

34. Alvarez-Ramirez, J.; Alvarez, J.; Rodríguez, E. Asymmetric long-term autocorrelations in crude oil markets. *Phys. A Stat. Mech. Its Appl.* **2015**, *424*, 330–341. [CrossRef]

35. Kassouri, Y. Boom-bust cycles in oil consumption: The role of explosive bubbles and asymmetric adjustments. *Energy Econ.* **2022**, *111*, 106006. [CrossRef]

36. Mensi, W.; Sensoy, A.; Vo, X.V.; Kang, S.H. Impact of COVID-19 outbreak on asymmetric multifractality of gold and oil prices. *Resour. Policy* **2020**, *69*, 101829. [CrossRef] [PubMed]

37. Arias-Calluari, K.; Najafi, M.N.; Harré, M.S.; Tang, Y.; Alonso-Marroquin, F. Testing stationarity of the detrended price return in stock markets. *Phys. A Stat. Mech. Its Appl.* **2022**, *587*, 126487. [CrossRef]

38. Su, X. Dynamic behaviors and contributing factors of volatility spillovers across G7 stock markets. *N. Am. J. Econ. Financ.* **2020**, *53*, 101218. [CrossRef]

39. Ghosh, B.; Bouri, E. Long memory and fractality in the universe of volatility indices. *Complexity* **2022**, *2022*, 6728432. [CrossRef]

40. Peng, C.K.; Buldyrev, S.V.; Havlin, S.; Simons, M.; Stanley, H.E.; Goldberger, A.L. Mosaic organization of DNA nucleotides. *Phys. Rev. E* **1994**, *49*, 1685–1689. [CrossRef] [PubMed]

41. Hochreiter, S.; Schmidhuber, J. Long Short-Term Memory. *Neural Comput.* **1997**, *9*, 1735–1780. [CrossRef] [PubMed]

42. Chung, J.; Gulcehre, C.; Cho, K.; Bengio, Y. Empirical Evaluation of Gated Recurrent Neural Networks on Sequence Modeling. *arXiv* **2014**, arXiv:1412.3555.

43. Luo, X.; Zhou, W.; Wang, W.; Zhu, Y.; Deng, J. Attention-Based Relation Extraction With Bidirectional Gated Recurrent Unit and Highway Network in the Analysis of Geological Data. *IEEE Access* **2018**, *6*, 5705–5715. [CrossRef]

44. Zhou, P.; Shi, W.; Tian, J.; Qi, Z.; Li, B.; Hao, H.; Xu, B. Attention-based bidirectional long short-term memory networks for relation classification. In Proceedings of the 54th Annual Meeting of the Association for Computational Linguistics (Volume 2: Short Papers), Berlin, Germany, 7–12 August 2016; pp. 207–212.

45. Lu, Q.; Zhu, Z.; Xu, F.; Zhang, D.; Wu, W.; Guo, Q. Bi-GRU Sentiment Classification for Chinese Based on Grammar Rules and BERT. *Int. J. Comput. Intell. Syst.* **2020**, *13*, 538–548. [CrossRef]

46. Diebold, F.X.; Mariano, R.S. Comparing Predictive Accuracy. *J. Bus. Econ. Stat.* **2002**, *20*, 134–144. [CrossRef]